Pharmaceutical Research, Vol. 23, No. 5, May 2006 (© 2006)
DOI: 10.1007/s11095-006-9904-6

Research Paper

Targeted High Lung Concentrations of Itraconazole Using Nebulized Dispersions in a Murine Model

Jason T. McConville,[1,5] Kirk A. Overhoff,[1] Prapasri Sinswat,[1] Jason M. Vaughn,[1] Bradi L. Frei,[1,2] David S. Burgess,[1,2,3] Robert L. Talbert,[1,2,3] Jay I. Peters,[3] Keith P. Johnston,[4] and Robert O. Williams III[1]

Received October 3, 2005; accepted December 23, 2005

Purpose. The purpose of this study was to investigate the delivery of itraconazole (ITZ) particles to a murine lung model by nebulization.
Methods. Three ITZ formulations were prepared and characterized in the dry state using contact angle, dissolution, X-ray powder diffraction, scanning electron microscopy, and Brunauer–Emmett–Teller surface area analysis. Aerodynamic particle size distributions and lung deposition studies in 14 outbred male ICR mice were performed using aqueous dispersions of all the formulations. A separate dosing uniformity study was also performed to qualify use of the chamber.
Results. All formulations had an aggregated particle size of approximately 30 μm in diameter. Two formulations showed that 80% of the drug dissolved in less than 5 min. The remaining ITZ formulation had a slower dissolution and the lowest total emitted dose from the nebulizer used. High concentrations of ITZ were shown to be present in the mouse lung during the lung deposition study, up to 16.8 ± 0.13 μg/g (± SE) were achieved. Concentrations of up to 0.76 ± 0.03 μg/g (± SE) could be maintained from the single nebulized dose for at least 24 h.
Conclusion. An effective method of targeted delivery of ITZ to the deep lung is presented that may be useful for the treatment and prevention of acute fungal infections.

KEY WORDS: antifungal; fungal infection; nanoparticle; nebulization; poorly water-soluble.

[1] College of Pharmacy, The University of Texas at Austin, Pharmaceutics PHR 4.214, 2409 W. University Avenue, Austin, Texas 78712-1074, USA.
[2] Department of Pharmacology, University of Texas Health Science Center at San Antonio, San Antonio, Texas 78229, USA.
[3] Department of Medicine, Division of Pulmonary Diseases/Critical Care Medicine, University of Texas Health Science Center at San Antonio, San Antonio, Texas 78229, USA.
[4] Department of Chemical Engineering, University of Texas at Austin, Austin, Texas 78712, USA.
[5] To whom correspondence should be addressed. (e-mail: jtmcconville@mail.utexas.edu)

ABBREVIATIONS: AIP, amorphous itraconazole powder; AIP-D, amorphous itraconazole powder dispersion; API, active pharmaceutical ingredient; AUC, area under the curve; BCS, Biopharmaceutical Classification System; BET, Brunauer–Emmett–Teller; BMT, bone marrow transplant; CIP, crystalline itraconazole powder; CIP-D, crystalline itraconazole powder dispersion; C_{max}, maximum concentration of drug; EPAS, evaporative precipitation into aqueous solution; GSD, geometric standard deviation; ITZ, itraconazole; λ, elimination rate constant of a noncompartmental analysis; MMAD, mass median aerodynamic diameter; %FPF, percent fine particle fraction; SEM, scanning electron microscopy; SFL, spray freezing into liquid; $T_{1/2}$, half-life of drug; T_{max}, time of maximum drug concentration; XRPD, X-ray powder diffraction.

INTRODUCTION

Systemic fungal infections are a major cause of morbidity and mortality in immunocompromised patient populations. Most common infections in this group are candidiasis and aspergillosis (1). Most recurring infections are caused by *Aspergillus* spp., which are responsible for 62% of acute invasive fungal infections. Following infection, mortality rates are as high as 49% for patients undergoing chemotherapy treatment for cancers such as leukemia and lymphoma, whereas patients with HIV/AIDS have one of the highest mortality rates at 86% (2). Lung transplant recipients belong to another extremely high-risk group; they are uniquely susceptible to infection because patients are intentionally maintained in an immunocompromized state and the lungs are constantly exposed to potential pathogens from the environment (3). Fatalities from aspergillosis are 74% within this group. All other transplant recipients are also at considerable risk for fungal infection, and bone marrow transplant (BMT) patients are at the highest risk with an 87% mortality rate upon infection.

In the United States alone, it was estimated that the direct cost of treating acute fungal infections was $2.6 billion

in 1998 (4). High costs of fungal therapy are directly related to the cost of individual therapy: A program of treatment for acute candidemia typically costs $40,000 per patient, whereas an infection of aspergillosis costs a staggering $72,000 per patient. Despite such a dismal prognosis for high-risk groups, frustratingly little improvement has been observed with the currently prescribed high-cost therapies.

The main route of infection for *Aspergillus* spp. is through the lung. Inhaled spores are able to germinate under the ideal conditions (e.g., high humidity, oxygen, and carbon dioxide) present in the lung (5,6). In the immunocompromised patient, there are few mechanisms to prevent this infection and growth; indeed, spores that are taken up by a reduced number of alveolar macrophages are typically able to germinate and propagate. At the macroscopic level, an *Aspergillus* spp. infection spreads within the lung parenchyma and invades vascular structures, resulting in bloodstream dissemination of the fungus to other vital organs throughout the host body (7,8).

Itraconazole (ITZ), a broad-spectrum triazole antifungal agent and a class II drug in the Biopharmaceutical Classification System (BCS), has poor bioavailability because of its poor solubility in water (<1 μg/mL). Currently used oral formulations of the drug must be given in high doses to achieve effective concentrations in the lungs to prevent germination of fungal spores. It is difficult to obtain suitable systemic concentrations of ITZ because of its poor and erratic absorption characteristics (9–11).

The mouse has previously been demonstrated to be a good model for small-scale inhalation studies, as the optimal particle size for deep lung exposure in both humans and mice is approximately 3 μm (12). A specially designed, restraint-free, small-animal inhalation dosing apparatus, as previously described, was selected for this study (13).

The primary objective of this study was to demonstrate that nanoparticles of ITZ, a poorly water-soluble active pharmaceutical ingredient (API), could be dispersed into aqueous liquid and nebulized effectively to the lung to provide potential prophylaxis and/or treatment against pulmonary aspergillosis. The secondary objective was to demonstrate that a nebulizer could deliver a uniform dose of ITZ to a study group of mice simultaneously dosed in the specially designed dosing chamber. As such, "Materials and methods" and "Results" are organized into two main sections. Section A deals with manufacture and characterization of powders containing ITZ by using either evaporative precipitation into aqueous solution (EPAS) or spray freezing into liquid (SFL) technologies. Section B focuses on the ITZ dispersions for nebulization by an investigation of the extent of particle dispersion *in vitro* required to provide an effective *in vivo* delivery. This demonstrates one type of inhalation delivery technique that could be used to deliver ITZ to the lung.

MATERIALS AND METHODS

The following materials were purchased: ITZ (Hawkins Chemical, Minneapolis, MN, USA); poloxamer 407, polysorbate 20, polysorbate 80, and sodium dodecyl sulfate (SDS) (Spectrum Chemicals, Gardena, CA, USA); diethanolamine (VWR International, West Chester, PA, USA); acetonitrile, dichloromethane, and methanol (EM Industries Inc., Gibbstown, NJ, USA); methoxyflurane (Pittman-Moore Inc., Mundelein, IL, USA); and normal saline (United States Pharmacopoeia (USP); Baxter, Deerfield, IL, USA).

Nanostructured ITZ Prepared using Either EPAS or SFL Technologies

EPAS is a technology for producing dispersions containing aggregates of nanoparticles (nanostructured aggregates) in aqueous solution (14). Briefly, ITZ (16% w/v) and poloxamer 407 (2.5% w/v) were dissolved in dichloromethane. The organic solution was heated and sprayed directly into an aqueous solution containing polysorbate 80 (2%), using the conditions indicated in Table I. A stabilized aqueous crystalline itraconazole powder dispersion (CIP-D; for nebulization)

Table I. Composition and Processing Parameters for Crystalline Dispersion (CIP-D) Prepared Using the EPAS Technique and Amorphous Powders (AIP1 and AIP2) Prepared Using the SFL Technique

Technique (formulation)	Ratio (composition)	Processing conditions
EPAS (CIP-D)	1:0.16:0.13 (ITZ/poloxamer 407/polysorbate 80)	Temperature of organic and aqueous solution = 80°C Spray flow rate = 1 mL/min (pressure drop = 20 MPa) Volume of receiving aqueous solution = 50 mL Spraying time = 6.25 min Final ITZ concentration = 20 mg/mL
SFL (AIP1)	1:1 (ITZ/polysorbate 20)	Tubing size = 10 cm × 63 mm ID polyether ether ketone (PEEK) Pump type = ISCO model 100DX syringe pump Constant pressure = 5000 psi Flow rate = 10–13 mL/min Spray media = liquid N_2
SFL (AIP2)	1:0.75:0.75 (ITZ/poloxamer 407/polysorbate 80)	As above with AIP1

EPAS, evaporative precipitation into aqueous solution; SFL = spray freezing into liquid and ITZ, itraconazole.

was formed at a nominal drug concentration of 20 mg/mL. A portion of CIP-D was quench-frozen in liquid nitrogen and lyophilized to yield a stabilized CIP of nanostructured particle aggregates. The CIP was then fully characterized as detailed in the following experimental sections.

Additionally, two stabilized amorphous itraconazole powder (AIP1 and AIP2) formulations were prepared using the SFL technology, as described previously (15). Briefly, for the amorphous powder composition 1 (AIP1), an organic feed solution was prepared by dissolving ITZ (0.1% w/v) and polysorbate 20 (0.1% w/v) into acetonitrile. For the second amorphous powder composition (AIP2), an organic feed solution was prepared by dissolving ITZ (0.1% w/v), polysorbate 80 (0.075% w/v), and poloxamer 407 (0.075% w/v) in acetonitrile. Each organic feed solution was atomized separately into liquid nitrogen to produce frozen amorphous particles using the conditions indicated in Table I. The frozen particles were lyophilized to isolate the stabilized AIP1 or AIP2 of nanostructured particle aggregates.

Section A: Investigation of Crystalline or Amorphous ITZ Powder Formulations

Scanning Electron Microscopy

Powdered samples (CIP, AIP1, or AIP2) were mounted on conductive tape and sputter coated using a model K575 sputter coater (Emitech Products, Inc., Houston, TX, USA) with gold/palladium for 35 s and viewed with a Hitachi S-4500 field emission scanning electron microscope (Hitachi High-Technologies Corp., Tokyo, Japan) with an accelerating voltage of 10–15 keV. Additionally, a portion of AIP2 (approximately 0.5 mg) was placed into a 0.2-mL PCR tube (Molecular BioProducts, Inc., San Diego, CA, USA) and 0.1 mL of epoxy resin was added while carefully avoiding the introduction of air into the sample. The AIP2 and resin were mixed using the handle of a cotton swab until the resin hardened; during this mixing, the resin became increasingly viscous, and an increasing shear was applied to the AIP2 sample until setting of the epoxy resin occurred. The resin sample was then placed in a 40°C oven overnight to cure. The sheared AIP2 set in resin was then sectioned using a razor blade and mounted onto conductive tape, sputter coated, and imaged as above.

Brunauer–Emmett–Teller Specific Surface Area Analysis

Specific surface area was measured using a Nova 2000 version 6.11 instrument (Quantachrome Instruments, Boynton Beach, FL, USA). Weighed powder (CIP, AIP1, or AIP2) was added to a 12-mm Quantachrome bulb sample cell and degassed for a minimum of 3 h. The data recorded were then analyzed using NOVA Enhanced Data Reduction Software (version 2.13) with the Brunauer–Emmett–Teller (BET) theory of surface area.

Dissolution Testing

Dissolution testing was performed on the powder samples (CIP, AIP1, or AIP2) using a USP 24 type II (paddle) apparatus (Model VK7000; Varian Inc., Palo Alto, CA, USA). An equivalent of 10 mg ITZ was added to 900 mL of dissolution medium (0.1 N HCl and 0.3% w/w SDS; pH 1.2). The dissolution medium was maintained at 37.0 ± 0.2°C, with a paddle speed of 50 rpm. Samples (5 mL) were withdrawn at 2, 5, 10, 20, 30, and 60 minute time intervals, filtered using a 0.45 μm GHP Acrodisc filter (Pall Corporation, East Hills, NY, USA), and analyzed using a Shimadzu LC-10 HPLC system (Shimadzu Corporation, Kyoto, Japan) equipped with an Alltech ODS-2 5 μm C-18 column (Alltech Associates, Inc., Deerfield, IL, USA). A mobile phase of acetonitrile/water/diethanolamine (70:30:0.05) at 1 mL/min eluted the ITZ peak at 5.5 min. The ITZ absorbance was measured at wavelength λ_{max} = 263 nm.

X-Ray Powder Diffraction

The X-ray diffraction patterns of the powders (CIP, AIP1, or AIP2) were analyzed using a Model 1710 X-ray Diffractometer (Philips Electronic Instruments, Inc., Mahwah, NJ, USA). Data were collected using primary monochromated radiation (CuKα1, λ = 1.54056 Å), a 2θ step size of 0.05, and a dwell time of 1.0 s per step.

Section B: Investigation of Dispersions for Nebulization

Filtration Study

Dispersions of AIP1 and AIP2 were prepared by adding an equivalent of 20 mg ITZ to 1 mL of deionized water (giving AIP1-D and AIP2-D at an equivalent of 20 mg/mL ITZ). To determine the portion of deaggregated particles that were less than 200 nm in size, the dispersions for nebulization (CIP-D, AIP1-D, or AIP2-D) were each passed through a 200-nm filter. For each dispersion, an aliquot of 1 mL (20 mg/mL ITZ equivalent) was passed through a preweighed 0.2 μm nylon membrane filter (Whatman Inc., Florham Park, NJ, USA) into a preweighed 1.5 mL centrifuge tube; this process was replicated to obtain concordant results. The filters and centrifuge tubes were allowed to dry overnight in a 60°C oven before cooling to room temperature and reweighing. The quantity of CIP, AIP1, or AIP2 that was retained on the filter (>200 nm) and the quantity of each formulation in the filtrate were determined (<200 nm).

Particle Size Analysis Using a Cascade Impactor

A 7 mL aliquot of the dispersions (CIP-D, AIP1-D, or AIP2-D at 20 mg/mL ITZ content) was dispensed into an Aeroneb® Pro micropump nebulizer (Aerogen Inc., Mountain View, CA, USA). Aerodynamic droplet size distributions were determined using a nonviable eight-stage cascade impactor (Thermo-Anderson, Symrna, GA, USA) to quantify total emitted dose (TED) per minute from the nebulizer output, mass median aerodynamic diameter (MMAD), geometric standard deviation (GSD), and percentage droplets with an aerodynamic diameter less than 4.7 μm (defined as the percentage fine particle fraction or %FPF).

Chamber Dosing Uniformity

Ten outbred male ICR mice were dosed with an amorphous ITZ formulation (AIP2-D) for 20 min using a

specially designed whole-body exposure unit, the design of which is described in a previous study (13). Briefly, the chamber consisted of a polymethylmethacrylate airtight box (40.6 × 11.4 × 21.6 cm) with a hinged top, having a nominal wall thickness of 1.25 cm. The chamber was designed to hold up to 14 mice, each having a floor area of approximately 63 cm^2, in accordance with The University of Texas at Austin and the University of Texas Health Science Center at San Antonio Institute of Animal Care and Use Committees (IACUCs) guidelines. An Aeroneb Pro micropump nebulizer was situated at the inlet of the chamber, and the drug was nebulized through the inlet into the chamber. Air was circulated from the chamber outlet, through a fan housing, back through the nebulizer into the chamber (at a flow rate of 1 L/min) to recirculate and maintain a high concentration of drug throughout. Following dosing, the mice were removed from the chamber and allowed to equilibrate for 15 min. The mice were euthanized, and the lungs (all lobes) were harvested from each animal.

Validated Lung Extraction and Analysis Using High-Performance Liquid Chromatography

Calibration standards and homogenized lung samples were analyzed using a previously published method (16). Briefly, normal saline (1 mL) was added to each harvested lung sample; this was then homogenized using tip ultrasonication. Aliquots of homogenate (250 μL) were transferred to four separate vials; 0.3 N barium hydroxide (50 μL) and 0.4 N zinc sulfate heptahydrate solution (50 μL) were then added to each vial to precipitate water-soluble proteins. The samples were then vortex mixed (30 s). Acetonitrile (1 mL) was added before a further vortex mixing (1 min), followed by centrifugation at 3000 × g (15 min). The supernatant was transferred to 1.5 mL centrifuge tubes and seated on an aluminum heating block (60°C) under a stream of nitrogen until dry.

Samples were reconstituted with 250 μL mobile phase (55% acetonitrile/35% water/10% methanol) and vortex mixed (1 min) before filtering (0.45 μm) into high-performance liquid chromatography (HPLC) injection vials with low volume inserts (250 μL). Each sample was analyzed using a Shimadzu LC-10 liquid chromatograph (Shimadzu Corporation) equipped with a heated (37°C) C-18 base-deactivated column (5 μm, 250 × 4.6 mm) protected by a C-18 guard column (5 μm, 7.5 × 4.6 mm) (Alltech Associates). The mobile phase eluted an ITZ peak at 20 min at a flow rate of 1.0 mL/min and an absorption wavelength of 263 nm (λ_{max}).

Lung Deposition Study

An animal study approved by the University of Texas at Austin and the University of Texas Health Science Center in San Antonio, Institutional Animal Care and Use Committees (IACUCs) was designed to determine the lung concentration and residence time of the ITZ formulations produced by the EPAS and SFL technologies. Three groups of outbred male ICR mice (14 per group) were dosed for 20 min in the dosing chamber (as outlined in the dosing uniformity study above), using 20 mg/mL dispersions of ITZ (CIP-D, AIP1-D, or AIP2-D). After dosing, mice were housed four per cage. At time points of 0.5, 1, 2, 4, 6, 10, and 24 h, two mice were removed and the lungs were harvested. Drug levels were determined for each time point using the validated HPLC analysis procedure (see above). A noncompartmental model was used to determine pharmacokinetic parameters for lung residence time using WinNonlin version 4.1 (Pharsight Corporation, Mountain View, CA, USA).

RESULTS

Section A: Investigation of Crystalline or Amorphous ITZ Powder Formulations

In Vitro Characterization

For the CIP particles obtained by quench freezing and drying, a crystalline dispersion of aggregated nanostructured particles was produced (Fig. 1). The aggregated structure resulting from the quench-freezing process was approximately 20–30 μm in size and was composed of smaller primary particles below 1 μm in size (nanoparticles).

The AIP1 particles displayed a different morphology compared with that of the CIP particles (Fig. 2A) as a result of the composition and processing technique. The large aggregated AIP1 particle, approximately 20 μm in diameter, seemed to have a relatively low surface area compared with that of CIP (BET surface area could not be obtained because of the high concentration of polysorbate 20, a liquid at room temperature). Higher magnification revealed that smaller particles seem to be embedded within a continuous surface (Fig. 2B). The polysorbate 20 may have been subject to spreading and coalescence during the lyophilization process prior to sputter coating for scanning electron microscopy (SEM) analysis, which would explain the continuous surface observed.

The AIP2 formulation displayed characteristics similar to the CIP formulation, as aggregated nanostructured particles with a high surface area were observed (Fig. 3A). Following the "shearing" preparation in the epoxy resin, it was clear that the large friable aggregated particle observed may easily be sheared and disrupted into smaller aggregated

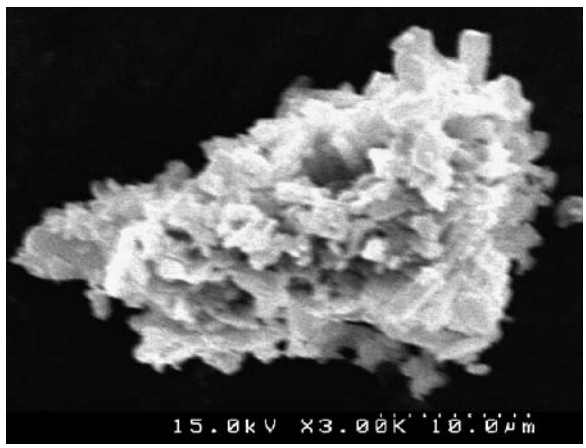

Fig. 1. Electron micrograph of aggregated nanoparticles of crystalline itraconazole powder (CIP) prepared using the EPAS process.

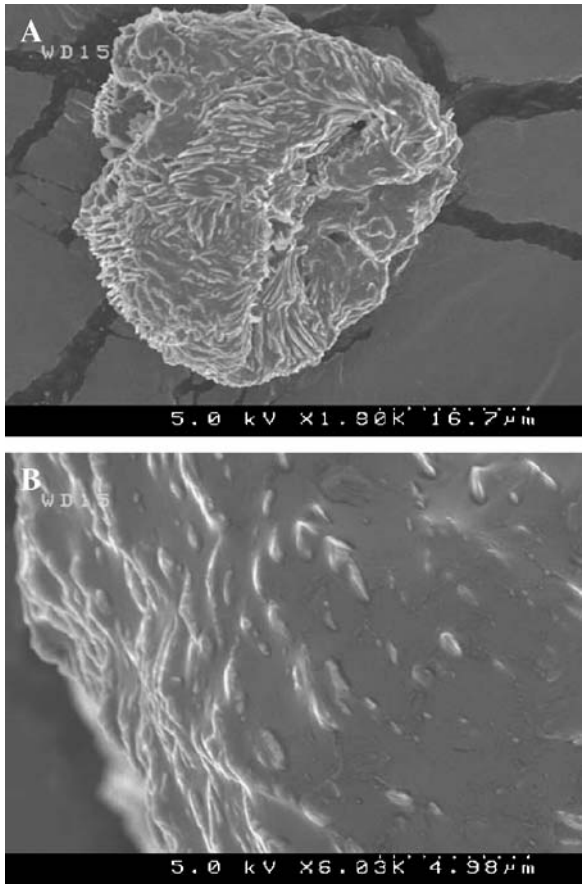

Fig. 2. Electron micrograph of aggregated nanoparticles of amorphous itraconazole powder (AIP1) prepared using the SFL process.

particles. The particle size of AIP2 was shown to vary from approximately 300 to 800 nm in diameter after this preparation step, as indicated (Fig. 3B).

BET Surface Area Analysis

The surface areas of CIP and AIP2 were determined to be 4.5 and 20 m^2/g, respectively. It was not possible to obtain a value for AP1 because of the high concentration of liquid polysorbate 20 in the composition.

Dissolution

Rapid dissolution rates were obtained for powders of CIP and AIP2, compared with the bulk ITZ material obtained from the manufacturer and that of AIP1 (Fig. 4). Both CIP and AIP2 demonstrate that 80% dissolution of drug was attained in less than 10 min. AIP1 displayed a release rate of approximately 80% within 30 min, as compared with approximately 50% for the bulk drug.

X-Ray Powder Diffraction

X-ray diffraction revealed that there was no detectable crystalline ITZ present in either of the samples (AIP1 or AIP2) produced using the SFL technology (Fig. 5), as previously reported for all formulations produced by this technology (15). For the EPAS-produced CIP sample, characteristic ITZ peaks were present, indicating the presence of crystalline drug, as seen previously for EPAS-produced powders (17). Broad peaks are observed in the AIP2 sample (2θ = 18–19°, and 2θ = 23–24°); these can be attributed to the poloxamer 407 in this formulation which has some degree of crystallinity following the lyophilization procedure (this was also observed for poloxamer alone, data not shown).

Section B: Investigation of Dispersed Powders for Nebulization

Filtration Study

After the CIP sample was passed through a 200 nm filter, only 14.4% of the sample was retained on the filter surface. Approximately 85% of the material was able to pass through the filter into a centrifuge tube. In the case of AIP2-D, 19.5% of the sample was retained on the filter surface. Approximately 80% of the material was able to pass through the filter into a centrifuge tube. For AIP1-D, however, only approximately 20% was able to pass through the filter, approximately 60% was retained by the filter, and the remaining 20% was observed to aggregate in the syringe and mixing vial and was unable to pass through the 200 nm syringe filter.

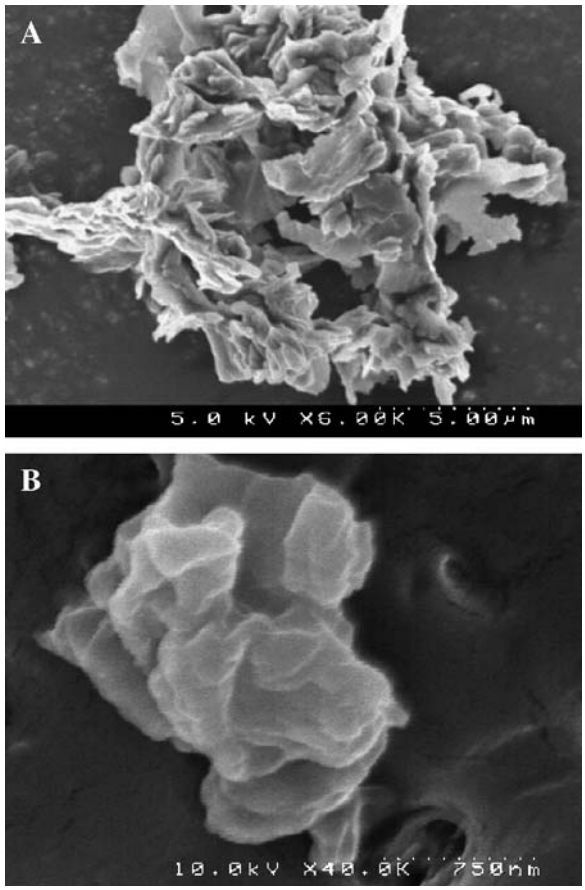

Fig. 3. (A) Electron micrographs of aggregated nanoparticles of amorphous itraconazole powder (AIP2) prepared using the SFL process and (B) AIP2-D following deaggregation in resin.

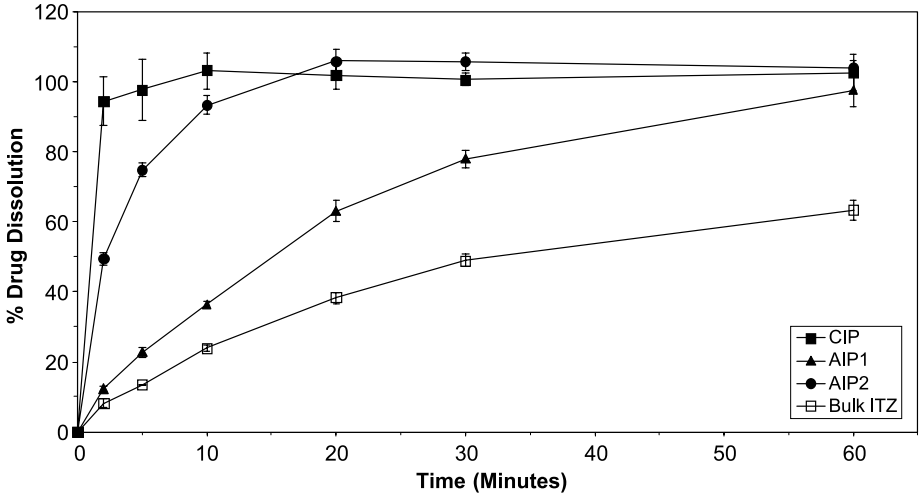

Fig. 4. Dissolution of nanoparticle formulations in 0.1 N HCl with 0.3% sodium lauryl sulfate, using USP II paddle apparatus at 50 rpm and 37°C.

Particle Size Analysis Using a Cascade Impactor

A summary of the cascade impactor data is provided in Table II. All formulations demonstrated reproducible MMADs and high %FPFs. The data indicated that formulation AIP1-D had the lowest TED per minute (417 μg) and the lowest FPF (71%). Alternatively, dispersions CIP-D and AIP2-D displayed TED values of 1743 and 1134 μg/min and %FPF values of 76 and 85%, respectively.

Chamber Dosing Uniformity

The variability of ITZ delivered to the lung was determined *in vivo* as a measurement of treatment efficiency and uniformity in dosing. Based on lung weights from each sacrificed mouse (wet lung weight), the ITZ delivered by inhalation attained an average concentration of 8.9 μg/g (SD = 1.16) wet lung weight (Fig. 6); error bars indicate the standard deviation obtained for each individual mouse (n = 4). Overall, the variation of the entire mouse population (n = 10) within the dosing chamber was only 13% relative standard deviation (RSD).

Lung Deposition Study

The highest lung concentration (C_{max}) of 16.8 μg/g was observed 30 min post dosing for nebulized CIP-D (Fig. 7). A low elimination rate constant (λ) of 0.10 h^{-1} for lung residence indicates that the dose was maintained at concentrations greater than 0.5 μg/g of lung tissue for up to 24 h (Table III). For the AIP2-D sample, a similar profile was observed, with a C_{max} of 13.4 μg/g at 1 h and a λ of 0.13 h^{-1}; the drug maintained a concentration greater than 0.75 μg/g for at least 24 h post-administration. The AIP1-D sample had a lower C_{max} (4.8 μg/g) and a higher elimination rate constant of 0.30 h^{-1}; as a result, the half-life was reduced to 2.3 h, and the drug concentration in the lungs was below the limit of detection at 10 h.

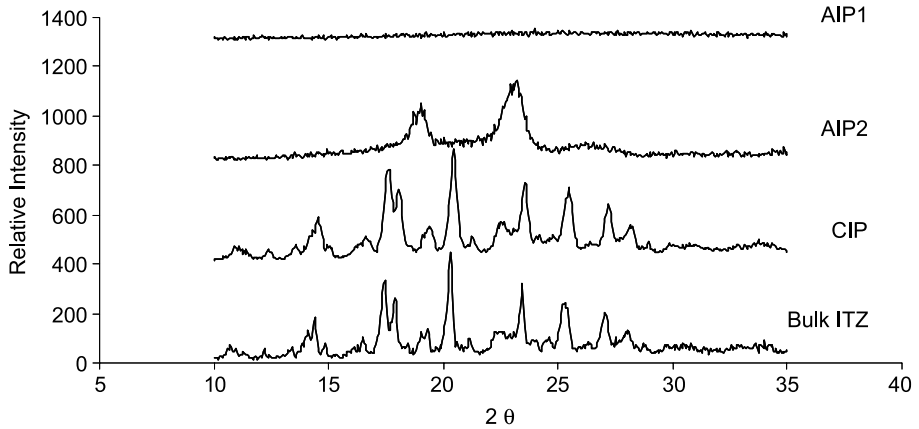

Fig. 5. X-ray powder diffraction of nanoparticle formulation crystalline powder (CIP) prepared using the EPAS technology, amorphous powder (AIP2) prepared using the SFL technology, and bulk micronized itraconazole (ITZ).

Table II. Cascade impactor data for crystalline dispersion (CIP-D) prepared using the EPAS technology, and amorphous dispersions (AIP1-D and AIP2-D) prepared using the SFL technology; aerosolized using the Aeroneb Pro micropump nebulizer.

Formulation	TED (μg/min)	FPF (%)	MMAD (μm)	GSD
CIP-D	1743	76	2.70	1.9
AIP1-D	417	71	2.76	2.1
AIP2-D	1134	85	2.82	1.7

DISCUSSION

Currently, there is no existing antifungal drug product available to treat the growing threat of acute pulmonary fungal infections by local targeting and deep lung deposition. To obtain a therapeutic level of drug at the site of lung infections, the maximum tolerable dose is typically orally administered to a patient. For ITZ, a poorly soluble drug, a high oral or intravenous dose must be administered, thus potentially increasing the incidence of unwanted side effects associated with a high drug serum concentration. In a previous article, it was reported that an ITZ serum concentration of 9 μg/mL (administered by oral gavage) was associated with a lung concentration of 2.5 μg/g (18). Local targeting of the drug at the usual site of infection (i.e., the lung) means that less total drug may be required for dosing and that the potential for side effects may be minimized due to a much reduced systemic concentration. Additionally, a targeted therapy may also initiate a quicker therapeutic onset and ultimately reduce the duration of treatment.

The SEM images of CIP and AIP2 indicated that the samples seemed to have large surface areas compared with that of AIP1. A large surface area and adequate surfactant coverage would be likely to facilitate dispersion into an aqueous medium prior to nebulization, thus allowing submicron particles to be incorporated into the nebulized droplets of 2–3 μm. Higher surface areas were obtained for the CIP and AIP2 when compared with the bulk ITZ powder. Previous data obtained using the SFL technology indicate that an appropriately large surface area was obtained for AIP2 (19). A surface area of AIP1 could not be obtained as it contained a high concentration of polysorbate 20 (a liquid at room temperature). The liquid polysorbate 20 spreads and covers sites on the solid preventing nitrogen gas adsorption, which is required for this type of measurement (observation of the SEM images suggested a low surface area). For the AIP1 formulation, it is likely that during the freezing process, the high surface area amorphous drug formed will be exposed to the liquid component (in this case polysorbate 20), causing the amorphous domains to swell. The polysorbate 20 adsorbed on the surface of the drug allows the drug molecules to have more diffusional mobility. The particles may then lose area due to coalescence of the highly mobile domains. This also has the potential to crystallize (not observed at the time of the X-ray analysis) (20). The SEM image of AIP1 reveals surface characteristics that might be attributed to a degree of melting in the SEM and would be consistent with mobility induced by the polysorbate 20.

The other amorphous formulation (AIP2) also had a polysorbate component (polysorbate 80), but this had a lower concentration than that contained within AIP1 due to the inclusion of the poloxamer 407 (Table I). A reduction in surface area was not apparent in this example. Smaller particles are liberated from the large aggregated nanostructured particles observed under the conditions present during the ultrasonication of the powder dispersions, a step prior to nebulization. Ultrasonication is considerably more vigorous than the low shear process applied simply by mixing the powders in the epoxy resin prior to imaging. Under these conditions, it is highly likely that the aggregated structures of CIP, AIP1, and AIP2 will be easily disrupted to liberate the nanosized drug-containing particles, and the presence of the surfactant in the nebulizer dispersion allows the disrupted particles to remain liberated. An extremely large surface is then exposed to the aqueous medium, enabling the predominantly nanosized dispersion of ITZ to be achieved prior to

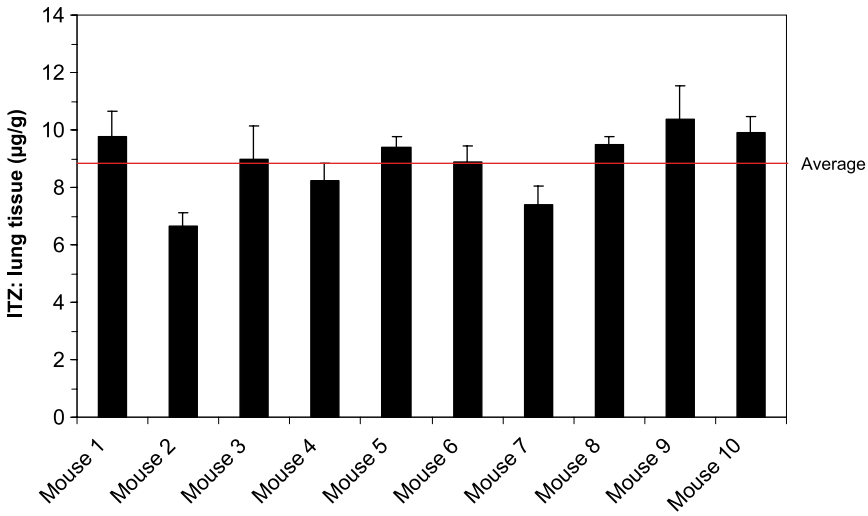

Fig. 6. Dosing uniformity of ten mice within the specially designed restraint-free whole-body exposure chamber. The formulation administered for nebulization was amorphous dispersion (AIP2-D) prepared using the SFL technology.

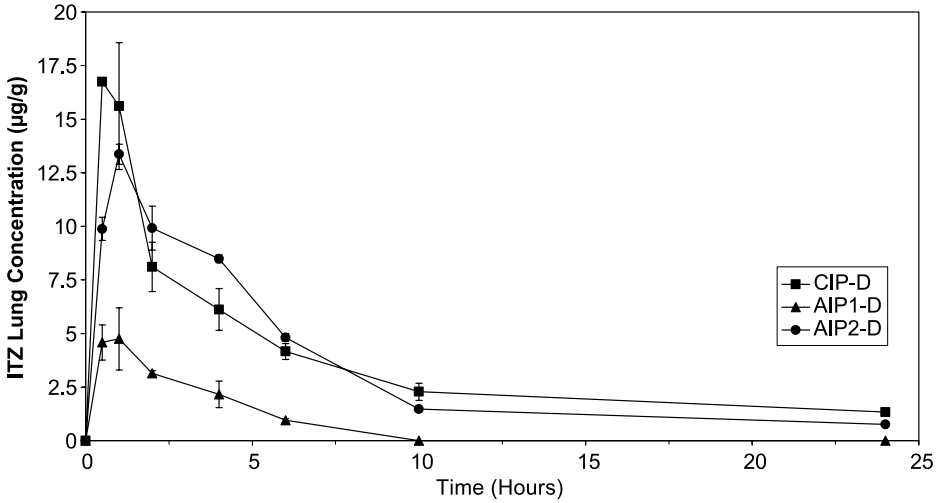

Fig. 7. Lung deposition in male outbred ICR mice (32 g) for nebulized ITZ formulations by single dose administration (an equivalent dose exposure of 30 mg/kg by aerosolization over a 20 minute period). The formulations administered for nebulization were crystalline dispersion (CIP-D) prepared using the EPAS technology, amorphous dispersion (AIP1-D) prepared using the SFL technology, and amorphous dispersion (AIP2-D) again prepared using the SFL technology.

nebulization; it may be assumed that the final particle size prior to nebulization is at least as small as those imaged by mixing in epoxy resin. It was clear that quite different morphologies were obtained from using the EPAS or SFL technologies in this example. In the case of EPAS, there was sufficient time available for crystal growth during the precipitation process, where growth can occur from the saturated solution of ITZ onto seeding particles. With the SFL process, the entire solvent solution was frozen in liquid nitrogen on a timescale of microseconds, resulting in a solid solution as described in a previous study (20). The solvent was then removed by lyophilization, and the solid component retains its amorphous morphology. It is well known that the larger chemical potential of an amorphous form of a drug raises its apparent solubility (21). It may be expected that rapid dissolution of ITZ from the SFL product can be then enhanced by the amorphous nature of the drug. However, because the crystalline EPAS formulation displays a more rapid dissolution than AIP2, other factors seemed to be important. In EPAS, the surfactant is directed to the surface of the drug during the particle formation. When comparing EPAS and SFL produced powders, drug in the SFL powder forms a solid solution with the surfactant and is thus not as concentrated at the surface of the particles, as in the case of EPAS (22). For the EPAS powder, it is likely that the intimate contact of this surfactant on the surface of the drug with the dissolution medium may have led to more rapid wetting than in the case of the SFL powders.

Additionally, at the time of dispersion of the powder samples, it is important that the chosen surfactant/stabilizer is able to promote wetting of the sample, allowing the particle to easily disperse. The aggregates (made up of nanostructured particles) produced by the various particle engineering technologies are held together primarily by electrostatic interaction in the dry powder form, as the particle charge-to-mass ratio is extremely high (23), as well as surfactant/stabilizer bridging between particles. Thin domains or macroscopic bridges between primary particles can be seen (Figs. 1 and 3A). Once the sample is in the dispersed state (in aqueous medium), it is important that there is sufficient surfactant/stabilizing excipient to overcome the attractive forces associated with the various particle interactions, which could ultimately lead to particle growth by flocculation, coalescence, and Ostwald ripening (24). Without the proper function of the surfactant/stabilizer, in this case polysorbate 20 or 80 and/or poloxamer 407, the particle aggregation/growth could potentially lead to poor functionality of the nebulizer, due to clogging of the micropump membrane, and an inability to form uniform dispersed droplets containing drug. Dissolution into an acidic medium allows some insight

Table III. Lung Deposition Pharmacokinetic Parameters for Crystalline Dispersion (CIP-D) Prepared Using the EPAS Process and Amorphous Dispersions (AIP1-D and AIP2-D) Prepared Using the SFL Process

Formulation	C_{max} (µg/g)	T_{max} (h)	$T_{1/2}$ (h)	λ (h^{-1})	$AUC_{(0-24)}$ (µg h/mL)	AUC_{inf} (µg h/mL)
CIP-D	16.8	0.5	6.7	0.10	86.8	99.7
AIP1-D	4.8	1	2.3	0.30	15.8	18.9
AIP2-D	13.4	1	5.5	0.13	79.8	85.8

AUC = area under the curve.

into the wettability of the various powder formulations and is significant when describing the type of dispersion that may occur when the powder is added to an aqueous medium to prepare the aqueous nebulizer dispersion. Given that the ITZ was processed to form nanostructured aggregates by using either EPAS or SFL technologies, then it is highly likely that the dissolution of ITZ will be rapid in an acidic medium (indeed, a dispersion of micronized ITZ with a mean particle size of 20 μm with 0.01% polysorbate 80 shows 100% dissolution in the same medium in less than 5 min; data not shown). The rate-limiting step for dissolution will not be the particle size, assuming each process resulted in nanostructured ITZ aggregates, but will be more related to the wettability of the formulation. Wetting is also very important to form a suitable dispersion of nanoparticles necessary for nebulization within droplets of 2–3 μm. In the case of AIP1, it was confirmed that although its dissolution was faster than that of the bulk ITZ drug, the apparent low surface area and probable poor surfactant distribution (based on the SEM images) would allow for poor initial wetting of this composition, hindering both wetting (the stage at which liberation of nanosized particles from the larger aggregated particle is important) and dissolution (which is initially dependent on the wettability of the large aggregated particle). For CIP and AIP2, dissolution profiles were more rapid, suggesting that the particles may have been more readily available to disperse and dissolve in the acidic medium. Visual observations agreed with the dissolution data, as clumping of AIP1 was seen on addition to the dissolution vessel. This was not apparent in the cases of CIP and AIP2, both exhibiting good dispersive properties (i.e., wettability) leading to rapid dissolution rates.

As indicated, the dissolution results suggested that AIP1 would have the poorest dispersion-forming properties (compared with CIP and AIP2); therefore, one might expect the poorest nebulization performance. Higher emitted dose values obtained for CIP-D and AIP2-D were also in agreement with the previous observations (SEM, BET, and dissolution), as compared with AIP1-D. The emitted dose was composed of 1- to 4-μm aqueous droplets, each containing a nanoparticle dispersion of ITZ, stabilized with surfactant and polymer. The quantity relating to the TED was dependent on the ability of the ITZ particles to disperse efficiently in the aqueous medium prior to nebulization. In the case of AIP1-D, although the %FPF was still quite high, the low TED was suggestive of particle aggregation within the nebulizer dosing reservoir. This may prevent the formation of a droplet by the nebulizer that contains a stable dispersion of nanosized ITZ particles. The Aeroneb Pro micropump nebulizer acts as a micropump by producing a fine spray of between 1- and 4-μm-sized droplets of the aqueous dispersion. The nebulizer was oriented so that the spray was produced at the bottom of the liquid reservoir, allowing droplets to form through a vibrating mesh design. Additionally, aggregates with "soft" polymer interconnects potentially break apart when passed through a vibrating mesh; this design provides a distinct advantage when attempting to nebulize dispersions. Traditional electronic nebulizer designs that rely on surface disruption and droplet formation (24) are unsuitable for dispersions, as they can potentially promote sedimentation within the nebulizer reservoir. Each prepared formulation has specific particle characteristics as a result of formulation design and processing. These specific particle characteristics may be optimized to provide desired properties for stability, long-term storage, packaging, patient compliance, and dosing regimens.

The material that passed through the filter was composed of ITZ, poloxamer 407 and polysorbate 80 (or ITZ polysorbate 20); it is reasonable to assume that only a small quantity of these highly water-soluble excipients would be retained on the filter. It is also reasonable to assume that a high proportion of the ITZ component is less than 200 nm in size and that the particles are suitable for dispersion in a nebulizer droplet. The SEM image (Fig. 3B) suggested that stabilized aggregated particles of ITZ (AIP2) could be deaggregated into discrete nanoparticles or smaller aggregates of nanoparticles that could be effectively aerosolized in a 2- to 5-μm nebulizer droplet, even before the addition of water to form the nebulizer dispersion (AIP2-D). Additionally, it is highly probable that the fraction of mass below 200 nm could be even higher than 80%, as sub-200-nm particles could build up a filter cake, slightly skewing the data. The data for CIP-D and AIP1-D were in agreement with the observation that CIP-D disperses as well as AIP2-D, and AIP1-D was not able to wet and disperse as effectively.

In the dosing uniformity experiment, each mouse displayed very similar lung concentration (per unit weight of wet lung tissue) with an RSD of only 13%. This may be considered a very acceptable variance considering physiological differences that could not be accounted for (i.e., breathing rate, mobility of each mouse, and their individual location within the dosing chamber over the specified 20 minute dosing exposure period). Additionally, it was observed that mice with a higher individual lung weight had a higher drug loading of ITZ, an observation consistent with an increased lung tidal volume. The low variability of the lung concentrations obtained demonstrated the validity of the dosing chamber as a uniform method to evaluate the effectiveness of pulmonary formulations. These data also highlight the effectiveness for delivery of the selected ITZ formulation to the deep lung.

A similar concentration (C_{max}) was found in the mouse lung for both the AIP2-D and CIP-D formulations post nebulization, and extremely high drug levels (greater than 0.5 μg ITZ/g lung weight) were observed for up to 24 h. Additionally, adequate lung concentration (C_{max} >2.5 μg/g) was observed for nebulized AIP1-D. The *in vivo* data presented were in direct agreement with the cascade impactor data and follow the same rank order: the AIP1-D formulation displaying the lowest C_{max} (4.75 μg/g) and the CIP-D formulation the highest C_{max} (16.8 μg/g). Both AIP2-D and CIP-D formulations displayed concentrations greater than 0.5 μg/g for at least 24 h (the final time point of the experiment). The extended drug half-lives for AIP2-D and CIP-D were likely to be caused by the poor aqueous solubility of ITZ, thus extending residence (greater than 24 h). The ITZ may be more removed from the lung either by macrophage uptake, dissolution, or a combination of these processes. The half-life for the AIP1-D formulation was markedly shorter than that obtained for AIP2-D and CIP-D. A logical explanation for this can be attributed to the improved dispersion prior to nebulization of the latter formulations. If the formulation is unlikely to disperse very well prior to nebulization, then the nebulized droplets themselves will contain larger particles of drug that are less

likely to reach the distal regions of the lung; they may then be cleared more rapidly by the mucociliary escalator in the upper airways of the lung. This is evidenced by the short half-life and higher elimination rate constant displayed for AIP1-D. Therapeutically, this is very important: To obtain lung levels greater than 0.5 μg/g of lung tissue, an extremely high and sustained dose of ITZ, considerably greater than used for a normal human dosing regimen, would be required by conventional oral delivery (18). In fact, the dose required using Sporanox® oral solution (one of the best methods of oral delivery of ITZ currently available in the market) to obtain the type of lung levels demonstrated by any of the pulmonary formulations presented in this paper would be likely to exhibit severe gastrointestinal symptoms (such as lethal diarrhea) in the animal model used. In all cases, single nebulized doses of the enhanced ITZ pulmonary formulations prepared using either the EPAS or SFL technologies were able to obtain elevated lung concentrations for extended periods of time.

Depending on the strain and severity of a fungal infection treatment, regimens of 200–800 mg ITZ b.i.d. or t.i.d. (25–31) are used, and a serum level greater than 0.5 μg/mL of the drug was considered to be important for successful therapy in some studies (30). The actual mass of drug available for deep lung deposition may be calculated by using the %FPF and the TED per minute; this reveals the order of deposition as CIP-D > AIP2-D > AIP1-D. The *in vivo* data were in good agreement with the data presented for the cascade impactor (particle size distribution and emitted dose), as the same rank order of drug available for deep lung deposition (FPF) is the same as the respective C_{max} values for the corresponding formulations (CIP-D > AIP2-D > AIP1-D).

CONCLUSIONS

The potential for an effective therapy of ITZ to reduce the mortality of immunocompromised patients has been clearly demonstrated with a lung deposition study in mice. High and sustained lung concentrations of nebulized ITZ demonstrate an effective method of delivery for local targeting to prevent fungal spore germination, growth, and dissemination of the fungus from the lung to the body. Stable forms of nanostructured aggregates of ITZ with varying surface properties can be prepared using a variety of nanoparticle technologies. A dry stabilized form of the drug may then be conveniently redispersed in an aqueous solution for nebulization. The size distribution of the aqueous droplets produced by the nebulizer is optimal for reaching the deep lung, whereas the high surface area of the dispersed particles within these droplets allows for rapid wetting and dissolution. The ability to decouple the size of the ITZ particles from the size of the nebulized droplets provides an advantage in achieving high concentrations in the deep lung for nanostructured drugs. This scheme provides an effective method for the delivery of a variety of poorly water-soluble drug candidates targeted to the deep lung.

ACKNOWLEDGMENTS

Acknowledgement for assistance in the *in vivo* study is given to Laura Najvar and John R. Graybill at The Division of Infectious Diseases at The University of Texas Health Science Center in San Antonio, Texas. The authors also acknowledge partial financial support from The Dow Chemical Company.

REFERENCES

1. M. Mendelson. Fungal infections in the immunocompromised. *Microbiol. Today* **28**:10–17 (2001).
2. S. J. Lin, J. Schranz, and S. M. Teutsch. Aspergillosis case—fatality rate: systematic review of the literature. *Clin. Infect. Dis.* **32**:358–366 (2001).
3. B. Mehrad, G. Paciocco, F. J. Martinez, T. C. Ojo, M. D. Iannettoni, and J. P. Lynch. Spectrum of *Aspergillus* infection in lung transplant recipients—case series and review of the literature. *Chest* **119**:169–175 (2001).
4. L. S. Wilson, C. M. Reyes, M. Stolpman, J. Speckman, K. Allen, and J. Beney. The direct cost and incidence of systemic fungal infections. *Value Health* **5**:26–34 (2002).
5. D. W. Denning. Invasive aspergillosis. *Clin. Infect. Dis.* **26**:781–803 (1998).
6. D. H. Griffin. Spore dormancy and germination. In D. H. Griffin (ed.), *Fungal Physiology*, Wiley, New York, 1994, pp. 375–398.
7. C. F. Pegues, E. S. Daar, and A. R. Murthy. The epidemiology of invasive pulmonary aspergillosis at a large teaching hospital. *Infect. Control Hosp. Epidemiol.* **22**:370–374 (2001).
8. P. Vaideeswar, S. Prasad, J. R. Deshpande, and S. P. Pandit. Invasive pulmonary aspergillosis: a study of 39 cases at autopsy. *J. Postgrad. Med.* **50**:21–26 (2004).
9. C. R. Bradford, A. G. Prentice, D. W. Warnock, and J. A. Copplestone. Comparison of the multiple dose pharmacokinetics of 2 formulations of itraconazole during remission induction for acute myeloblastic-leukemia. *J. Antimicrob. Chemother.* **28**:555–560 (1991).
10. G. Vreugdenhil, B. J. Vandijke, J. P. Donnelly, I. R. O. Novakova, J. M. M. Raemaekers, M. A. A. Hoogkampkorstanje, M. Koster, and B. E. Depauw. Efficacy of itraconazole in the prevention of fungal-infections among neutropenic patients with hematologic malignancies and intensive chemotherapy—a double-blind, placebo-controlled study. *Leuk. Lymphoma* **11**:353–358 (1993).
11. D. Smith, V. Vandevelde, R. Woestenborghs, and B. G. Gazzard. The pharmacokinetics of oral itraconazole in AIDS patients. *J. Pharm. Pharmacol.* **44**:618–619 (1992).
12. F. J. Miller, R. R. Mercer, and J. D. Crapo. Lower respiratory-tract structure of laboratory-animals and humans—dosimetry implications. *Aerosol Sci. Technol.* **18**:257–271 (1993).
13. J. T. McConville, T. C. Carvalho, A. N. Iberg, R. L. Talbert, D. S. Burgess, J. I. Peters, K. P. Johnston, and R. O. Williams III. Design and evaluation of a restraint-free small animal inhalation dosing chamber. *Drug Dev. Ind. Pharm.* **31**:35–42 (2005).
14. J. H. Hu, K. P. Johnston, and R. O. Williams III. Nanoparticle engineering processes for enhancing the dissolution rates of poorly water soluble drugs. *Drug Dev. Ind. Pharm.* **30**:233–245 (2004).
15. J. H. Hu, K. P. Johnston, and R. O. Williams III. Stable amorphous danazol nanostructured powders with rapid dissolution rates produced by spray freezing into liquid. *Drug Dev. Ind. Pharm.* **30**:695–704 (2004).
16. P. O. Gubbins, B. J. Gurley, and J. Bowman. Rapid and sensitive high performance liquid chromatographic method for the determination of itraconazole and its hydroxy-metabolite in human serum. *J. Pharm. Biomed. Anal.* **16**:1005–1012 (1998).
17. X. Chen, Z. Benhayoune, R. O. Williams III, and K. P. Johnston. Rapid dissolution of high potency itraconazole particles produced by evaporative precipitation into aqueous solution. *J. Drug Del. Sci. Technol.* **14**:299–304 (2004).
18. R. Allendoerfer, D. Loebenberg, M. G. Rinaldi, and J. R. Graybill. Evaluation of SCH51048 in an experimental-model of pulmonary aspergillosis. *Antimicrob. Agents Chemother.* **39**:1345–1348 (1995).
19. J. H. Hu, K. P. Johnston, and R. O. Williams III. Spray freezing into liquid (SFL) particle engineering technology to enhance dissolution of poorly water soluble drugs: organic solvent versus

organic/aqueous co-solvent systems. *Eur. J. Pharm. Sci.* **20**: 295–303 (2003).
20. J. M. Vaughn, X. Gao, M.-J. Yacaman, K. P. Johnston, and R. O. Williams III. Comparison of powder produced by evaporative precipitation into aqueous solution (EPAS) and spray freezing into liquid (SFL) technologies using novel Z-contrast STEM and complimentary techniques. *Eur. J. Pharm. Biopharm.* **60**:81–89 (2005).
21. S. D. Yoo, S. H. Lee, E. H. Kang, H. Jun, J. Y. Jung, J. W. Park, and K. H. Lee. Bioavailability of itraconazole in rats and rabbits after administration of tablets containing solid dispersion particles. *Drug Dev. Ind. Pharm.* **26**:27–34 (1999).
22. M. Sarkari, J. Brown, X. X. Chen, S. Swinnea, R. O. Williams III, and K. P. Johnston. Enhanced drug dissolution using evaporative precipitation into aqueous solution. *Int. J. Pharm.* **243**:17–31 (2002).
23. J. Baxter, H. Abou-Chakra, U. Tuzun, and B. M. Lamptey. A DEM simulation and experimental strategy for solving fine powder flow problems. *Chem. Eng. Res. Des.* **78**:1019–1025 (2000).
24. P. P. H. Le Brun, A. H. de Boer, H. G. M. Heijerman, and H. W. Frijlink. A review of the technical aspects of drug nebulization. *Pharm. World Sci.* **22**:75–81 (2000).
25. J. Wheat, G. Sarosi, D. McKinsey, R. Hamill, R. Bradsher, P. Johnson, J. Loyd, and C. Kauffman. Practice guidelines for the management of patients with histoplasmosis. *Clin. Infect. Dis.* **30**:688–695 (2000).
26. C. A. Kauffman, R. Hajjeh, and S. W. Chapman. Practice guidelines for the management of patients with sporotrichosis. *Clin. Infect. Dis.* **30**:684–687 (2000).
27. S. W. Chapman, R. W. Bradsher, G. D. Campbell, P. G. Pappas, and C. A. Kauffman. Practice guidelines for the management of patients with blastomycosis. *Clin. Infect. Dis.* **30**:679–683 (2000).
28. J. H. Rex, T. J. Walsh, J. D. Sobel, S. G. Filler, P. G. Pappas, W. E. Dismukes, and J. E. Edwards. Practice guidelines for the treatment of candidiasis. *Clin. Infect. Dis.* **30**:662–678 (2000).
29. J. N. Galgiani, N. M. Ampel, A. Catanzaro, R. H. Johnson, D. A. Stevens, and P. L. Williams. Practice guidelines for the treatment of coccidioidomycosis. *Clin. Infect. Dis.* **30**:658–661 (2000).
30. J. D. Sobel. Practice guidelines for the treatment of fungal infections. *Clin. Infect. Dis.* **30**:652, (2000).
31. P. G. Pappas, J. H. Rex, J. D. Sobel, S. G. Filler, W. E. Dismukes, T. J. Walsh, and J. E. Edwards. Guidelines for treatment of candidiasis. *Clin. Infect. Dis.* **38**:161–189 (2004).